FULL PAPER

BJC

British Journal of Cancer (2015) 113, 433–442 | doi: 10.1038/bjc.2015.229

Keywords: gastric cancer; suppressor of cytokine signalling; ataxia telangiectasia and Rad3-related protein; cell cycle arrest; adenovirus vector; gene therapy; peritoneal carcinomatosis

Gene therapy with SOCS1 for gastric cancer induces G2/M arrest and has an antitumour effect on peritoneal carcinomatosis

Rie Natatsuka[1,2], Tsuyoshi Takahashi*[,1,2], Satoshi Serada[2], Minoru Fujimoto[2], Tomohiro Ookawara[2], Toshirou Nishida[3], Hisashi Hara[1,2], Takahiko Nishigaki[1,2], Emi Harada[2], Takashi Murakami[4], Yasuhiro Miyazaki[1], Tomoki Makino[1], Yukinori Kurokawa[1], Makoto Yamasaki[1], Hiroshi Miyata[1], Kiyokazu Nakajima[1], Shuji Takiguchi[1], Tadamitsu Kishimoto[5], Masaki Mori[1], Yuichiro Doki[1] and Tetsuji Naka*[,2]

[1]Department of Gastroenterological Surgery, Osaka University Graduate School of Medicine, 2-2 E2, Yamadaoka, Suita city, Osaka, 565-0871, Japan; [2]Laboratory for Immune Signal, National Institute of Biomedical Innovation, 7-6-8 Saito-Asagi, Ibaraki city, Osaka, 567-0085, Japan; [3]Department of Surgery, National Cancer Center Hospital East, 6-5-1 Kashiwanoha, Kashiwa city, Chiba, 277-8577, Japan; [4]Department of Pharmacy, Takasaki University of Health and Welfare, 37-1 Nakaorui-machi, Takasaki city, Gunma 370-0033, Japan and [5]Laboratory of Immune Regulation, Immunologu Frontier Research Center, Osaka University, 3-1 Yamadaoka, Suita city, Osaka, 565-0871, Japan

Background: Suppressor of cytokine signaling1 (SOCS1) is a negative regulator of various cytokines. Recently, it was investigated as a therapeutic target in various cancers. However, the observed antitumour effects of SOCS1 cannot not be fully explained without taking inhibition of proliferation signalling into account. Our aim was to discover a new mechanism of antitumour effects of SOCS1 for gastric cancer (GC).

Methods: We analysed the mechanism of antitumour effect of SOCS1 *in vitro*. In addition, we evaluated antitumour effect for GC using a xenograft peritoneal carcinomatosis mouse model in preclinical setting.

Results: We confirmed that SOCS1 suppressed proliferation in four out of five GC cell lines. SOCS1 appeared to block proliferation by a new mechanism that involves cell cycle regulation at the G2/M checkpoint. We showed that SOCS1 influenced cell cycle-associated molecules through its interaction with ataxia telangiectasia and Rad3-related protein. The significant difference in therapeutic effects was noted in terms of the post-treatment weight and total photon count of the intra-abdominal tumours.

Conclusion: Forced expression of SOCS1 revealed a heretofore-unknown mechanism for regulating the cell cycle and may represent a novel therapeutic approach for the treatment of peritoneal carcinomatosis of GC.

Gastric cancer (GC) is the fourth most common cancer and the second most common cause of cancer-related deaths (Parkin *et al*, 2005; Ferlay *et al*, 2010; Fujiwara *et al*, 2012). Peritoneal carcinomatosis (PC) is the most frequent mode of recurrence and is responsible for about 60% of all deaths from GC (Maruyama *et al*, 2006). Peritoneal carcinomatosis develops from micro metastases that originate from free cancer cells seeded from a primary gastric tumour. It causes bowel obstruction and cancerous ascites and gradually decreases the quality of life of patients. GC patients with PC are considered to be noncurable and are usually treated with systemic chemotherapy without surgical resection. Although recent randomised clinical trials have proposed several standards for combination chemotherapy for incurable GC (Van Cutsem *et al*, 2006; Koizumi *et al*, 2008; Pasini *et al*, 2011),

*Correspondence: Dr T Takahashi; E-mail: ttakahashi2@gesurg.med.osaka-u.ac.jp or Dr T Naka; E-mail: tnaka@nibio.go.jp

Revised 18 May 2015; accepted 21 May 2015; published online 16 July 2015

the median survival times associated with these regimens are about 12 months; thus, a new and multidisciplinary approach to GC is needed.

The suppressor of cytokine signalling (SOCS) family, characterised by a central src homology 2 domain and a conserved C-terminal SOCS box, is composed of eight structurally related proteins (Fujimoto and Naka, 2003). Of these, SOCS1 is known as the most potent negative regulator of proinflammatory cytokine signalling. It interacts with phosphotyrosine residues on proteins such as JAK kinases to interfere with the activation of STAT proteins or other signalling intermediates (Watanabe *et al*, 2004; Iwahori *et al*, 2013; Shimada *et al*, 2013). Inactivation of the SOCS1 gene was reported to have a possible association with oncogenesis of GC, and the signalling pathways targeted by SOCS1 are important for GC cell proliferation (Oshimo *et al*, 2004; To *et al*, 2004). We previously reported that SOCS1 is silenced in GC cell lines, and that it is involved in enhanced STAT3 activation in these cells (Souma *et al*, 2012). We also demonstrated that gene delivery of SOCS1 in GC cells has a potent antiproliferative effect via the suppression of not only JAK/STAT activation, but also inhibition of p38 MAPK signalling. Moreover, we found that overexpression of SOCS1 may have a stronger effect than that of various kinase inhibitors in GC cells; thus, the potent antiproliferative effect of SOCS1 must depend not only on proliferative signal inhibition but also on an as-yet unknown mechanism.

There have been few reports about the association between SOCS1 and cell cycle progression. Suppressor of cytokine signaling proteins direct the turnover of cellular targets through the formation of a complex with the Elongin-Cullin E3 ligase complex. In this way, SOCS modulates the ubiquitination of a variety of proteins, which are subsequently recognised by the proteasome and degraded. Parrillas *et al* (2013) previously reported that SOCS1 is associated with degradation of Cdh1 and blockades melanoma cells in mitosis by G2/M arrest via regulation of cyclin D and cyclin E. G1/S arrest was also reported in melanoma cells treated with a JAK inhibitor and was associated with reduced STAT3 activation (Xu *et al*, 2015). In the present study, we found that SOCS1 had cell cycle inhibitory activity at the G2/M phase in GC cells. Our aim was to clarify the role of the unknown, cell cycle-associated mechanism of SOCS1 in GC cells by enforced SOCS1 expression with an adenoviral vector (AdSOCS1). We also evaluated a new treatment strategy that used the adenovirus to incorporate SOCS1 into PC cells.

MATERIALS AND METHODS

Cell lines. The following human GC cell lines were obtained from the Japanese Collection of Research Bioresources (Osaka, Japan): MKN45 (JCRB0254); the luciferase stably expressing cell line MKN45-Luc (JCRB1379), NUGC-2 (JCRB0821), OCUM-1 (JCRB0192), and KATO-III (JCRB0611). AGS was purchased from the American Type Culture Collection (Manassas, VA, USA). Cell line identities were confirmed by DNA fingerprinting through short tandem repeat profiling.

Preparation of adenoviruses. A replication-defective recombinant adenoviral vector expressing the mouse SOCS1 gene (AdSOCS1) was provided by Dr. Hiroyuki Mizuguchi (Osaka University, Osaka, Japan); this vector was constructed with an improved *in vitro* ligation method, as described previously (Mizuguchi and Kay, 1999). An adenoviral vector expressing the LacZ gene (AdLacZ) was constructed by a similar method, and the expression of these genes was regulated by means of a CMV promoter/enhancer and intron A.

Antibodies. The following primary antibodies were obtained from Cell Signaling Technology (Danvers, MA, USA): anti-phospho-STAT3 (Tyr705; 1:1000), anti-cleaved caspase3 (1:1000), anti-phospho-Chk2 (Thr68; 1:1000), anti-Chk2 (1:1000), anti-phospho-cdc2 (Tyr15; 1:1000), anti-phospho-cdc2 (Thr161; 1:1000), anti-cdc2 (1:1000), anti-phospho-cdc25C (Thr48; 1:1000), anti-cdc25C (1:1000), and anti-cyclinB1 (1:1000). Anti-STAT3 (1:1000), anti-GAPDH (1:2000), and anti-ataxia telangiectasia and Rad3-related protein (ATR) (1:1000) antibodies were obtained from Santa Cruz Biotechnology (Santa Cruz, CA, USA), and anti-SOCS1 (1:1000) antibody was obtained from IBL (Fujioka, Gunma, Japan).

Western blotting. Cells were lysed in radioimmunoprecipitation assay buffer (10 mM Tris-HCl pH 7.5, 150 mM NaCl, 1% Nonidet P-40, 0.5% sodium deoxycholate, 0.1% SDS, 1% protease-inhibitor cocktail, and 1% phosphatase-inhibitor cocktail). Following centrifugation (16 100 rcf, at 4 °C, 15 min), soluble proteins in the supernatant were obtained. Extracted proteins were resolved using SDS-PAGE gels (Wako Pure Chemical Industries, Osaka, Japan). After transfer of the proteins to PVDF membranes (Millipore, Bedford, MA, USA), the membranes were washed and blocked with 1% bovine serum albumin (Nacalai Tesque, Kyoto, Japan) in PBS containing 0.1% Tween 20 (PBST) or 5% non-fat dry milk (Cell Signaling Technology) in PBS containing 0.1% Tween 20 (TBST). Membranes were incubated with the respective antibodies against different targets. Antibodies and their dilution ratios were previously shown. Next, the membranes were incubated with horseradish peroxidase-conjugated sheep anti-rabbit IgG (GE Health-care, Little Chalfont, Buckinghamshire, UK) or horseradish peroxidase-conjugated donkey anti-goat IgG (Santa Cruz). Finally, the signals were visualised by means of an ECL reaction system (Perkin Elmer Life Science, Boston, MA, USA).

Co-immunoprecipitation (Co-IP). MKN45 cells were infected with AdLacZ or AdSOCS1 (40 multiplicity of infection). Twenty-four hours post infection, to prepare cell lysates, cells were washed twice with PBS and collected by scraping in cold radioimmunoprecipitation assay buffer with 1% protease-inhibitor cocktail and 1% phosphatase-inhibitor cocktail after 5 min of incubation on ice. Co-immunoprecipitation was performed with 1 mg of total cell proteins overnight at 4 °C with anti-ATR antibody (N-19, 1:200; Santa Cruz Biotechnology).

Immunoprecipitates were recovered by 1 h of incubation at 4 °C with Protein G Sepharose 4 Fast Flow (GE Healthcare, Little Chalfont, Buckinghamshire, UK). Precipitates were washed five times with cold radioimmunoprecipitation assay buffer, eluted in 30 μl of 2 × SDS sample buffer, and boiled for 5 min. Half of each elution (15 μl) was separated by SDS-PAGE and transferred to PVDF membranes.

Proliferation assay. Cells were seeded into 96-well plates at 3000 cells per well (Costar; Corning Inc., Corning, NY, USA) for 24 h, and then treated with AdLacZ or AdSOCS1 (0–160 multiplicity of infection) for 48 h. Cell proliferation was evaluated with the WST-8 (2-(2-methoxy-4-nitrophenyl)-3-(4-nitrophenyl)-5-(2,4-disulfophenyl) -2H-tetrazolium, monosodium salt) assay (Cell Counting Kit-SF; Nacalai Tesque) at the indicated post-treatment times. Microplate reader Model 680 (Bio-Rad Laboratories, Hercules, CA, USA) was used to measure WST-8 absorption at a wavelength of 450 nm with a reference wavelength of 630 nm. Growth rate was expressed as the percentage of absorbance for treated cells *vs* control cells as described previously (Takahashi *et al*, 2013). Experiments were performed at least in triplicate, of which the values are the averages of triplicate wells.

Caspase-3 activity assay. Each cell line was seeded into six-well plates at a density of 3×10^5 cells per well and treated with AdLacZ or AdSOCS1 for 2 days. The cells were then washed with PBS, and caspase-3 activity was detected with a caspase-3 fluorometric assay kit (R&D systems, Minneapolis, MN, USA) according to the manufacturer's instructions.

siRNA knockdown. Short interfering RNA (siRNA) ON-TARGET Plus SMART pools were purchased from Thermo Scientific Dharmacon (Yokohama, Kanagawa, Japan): nontargeting (D-001810-10-20) and ATR (L-003202-00-0010). Approximately 1.0×10^5 cells per well were seeded into 12-well plates with 1 ml of antibiotic-free RPMI 1640 medium with 10% FBS. The next day, cells were transfected with nontargeting or ATR siRNA using Lipofectamine RNAiMAX transfection reagent (Invitrogen, Carlsbad, CA, USA) according to the manufacturer's instructions. After 24 h, cells were treated with AdLacZ or AdSOCS1 (160 multiplicity of infection) and incubated. For cell cycle analysis, cells were incubated for 24 h, and for western blotting analysis, cells were incubated for 48 h.

Cell cycle analysis. Gastric cancer cell lines were infected with 160 multiplicity of infection AdLacZ or AdSOCS1 for 24 h. Cells were harvested and stained with Cycletest Plus DNA Reagent Kit (BD: BD Biosciences, San Jose, CA, USA) according to the manufacturer's instructions. The various cell cycle phases were monitored with a FACS Canto II flow cytometer (BD Biosciences) and analysed using FlowJo software ver.8.8.7 (Treestar, Inc., San Carlos, CA, USA).

Mouse xenograft model. All animal experiments were approved by the animal research committee of the National Institute of Biomedical Innovation (Osaka, Japan) and conducted according to the institutional ethical guidelines for animal experimentation. Female ICR nu/nu mice, 4 weeks old, were obtained from Charles River Japan (Yokohama, Japan). For peritoneal dissemination xenograft experiments, the luciferase stably expressing cell line MKN45-Luc was selected. Starting at 3 weeks after cell inoculation, bioluminescence imaging was performed to select peritoneal dissemination xenograft mice, and thereafter every 14 days to monitor tumour progression. The mice were intraperitoneally injected with 1×10^8 pfu per 500 μl of AdSOCS1 or AdLacZ twice a week a total of eight times starting 3 weeks after the implantation of MKN45-Luc cells into the abdominal space. After 49 days of tumour cell inoculation, the mice were killed and their abdominal spaces examined macroscopically for growths. Tumours detected in the abdominal spaces were removed and weighed.

***In vivo* imaging system.** VivoGloTM Luciferin, *In Vivo* Grade (Promega, Madison, WI, USA) was resuspended in PBS to a concentration of 150 mg ml^{-1} and filter-sterilised through a 0.2-μm filter. Each mouse was intraperitoneally injected with 10 μl per gram of body weight with 23-gauge needles. Mice were anaesthetised by the XGI-8 Gas Anesthesia system (2% isoflurane; Xenogen, Alameda, CA, USA), and 20 and 25 min after injection of luciferin, luciferase activity was detected by *In Vivo* Imaging System (IVIS) Lumina (Xenogen). To acquire an image sequence, we used Living Image Ver.2.6 (Xenogen) image software; the region of interest was drawn as the whole abdominal area, and we measured the photon flux data as described previously (Toyoshima *et al*, 2009).

Immunohistochemistry. Peritoneal implanted tumours were harvested and paraffin-embedded for immunohistochemical analysis using anti-SOCS1 antibody (Abcam, Cambridge, MA, USA) and anti-Ki-67 antibody (Novocastra Laboratories, Newcastle, UK). A TUNEL assay (with DAPI nuclear counterstaining) for apoptosis was carried out using the ApopTag Fluorescein *In Situ* Apoptosis Detection Kit (Chemicon International, Temecula, CA, USA) according to the manufacturer's instructions.

Statistical analysis. Experiments with cell lines were repeated at least three times. Statistical analyses were performed using Welch's *t*-test and Mann–Whitney *U* test. Two-sided *P* values less than 0.05 were considered significant. These analyses were carried out using JMP version 11.0 (SAS Institute, Cary, NC, USA) for Windows.

RESULTS

SOCS1 gene delivery associated with marked antiproliferative effects in several GC cell lines. Because poorly differentiated GC types have a high risk of recurrence, including peritoneal dissemination, we selected MKN45, AGS, KATO-III, NUGC2, and OCUM-1 cell lines, which have been shown to be poorly differentiated adenocarcinoma GC cell lines. We found that SOCS1 gene delivery using an adenoviral vector suppressed the proliferation of four out of the five cell lines in a proliferation assay (Figure 1A). In particular, proliferation of MKN45, AGS, and KATO-III were inhibited in a dose-dependent manner. To evaluate the molecular pathway of apoptosis induced by SOCS1, we measured the level of caspase-3 activity using specific fluorogenic peptide substrates after infection with each adenovirus vector. As shown in Figure 1B, the level caspase-3 activation was significantly higher in AdSOCS1-treated cells; these results indicate that SOCS1 was involved in the activation of caspase-3-mediated apoptosis.

Effect of SOCS1 on JAK/STAT3 pathways. We next determined the activation status of signalling molecules in GC cells infected with AdLacZ or AdSOCS1. Immunoblotting analysis showed that phosphorylation levels of STAT3 were effectively decreased in MKN-45 (Figure 1C) and AGS (data not shown) cells treated with AdSOCS1. In addition, forced expression of SOCS1 was associated with increased expression of cleaved caspase-3, as revealed by western blotting (Figure 1C).

Induction of cell cycle arrest at the G2/M phase by SOCS1. Next, we used flow cytometry to investigate the effect of SOCS1 on cell cycle progression. Compared with controls, overexpression of SOCS1 increased the ratio of cells in the G2/M phase in all three GC cell lines (Figure 2A and B) Our results indicate that SOCS1 affected the G2/M check-point; however, little is known about the role of SOCS1 in cell cycle regulation. To determine the molecular basis of the SOCS1-induced G2/M transition blockade, we analysed SOCS1-transfected MKN-45 cells and control cells by western blotting using monoclonal antibodies specific for several key regulators, including Chk-2, p-Chk2 (Thr68), cdc25c, p-cdc2 (Tyr161), p-cdc2 (Tyr15), and cyclin B. SOCS1-transfected MKN-45 cells showed a notable increase in p-Chk2 (Thr68) and p-cdc25c (Thr48) levels, whereas Chk2 and cdc25c levels were unchanged compared with controls (Figure 2C). Furthermore, SOCS1-transfected MKN-45 cells showed a notable decrease in p-cdc2 (Tyr161) and p-cdc2 (Tyr15) (Figure 2C). Figure 2D shows a schema of the relationships among key molecules involved in the G2/M checkpoint. Suppressor of cytokine signaling1 induced phosphorylation of Chk2 (Thr68) and cdc25C (Thr48). Phosphorylation of cdc25c (Thr48) suppressed cdc2 (Tyr15) and cdc2 (Tyr161).

SOCS1 interacts with ATR to induce Chk2 to phosphorylate and trigger G2/M phase arrest. To clarify the mechanism between SOCS1 and phosphorylation of Chk2, we examined the association between SOCS1 and ATR, which was reported to bind SOCS1 through the SOCS box and p53 (Calabrese *et al*, 2009; Mallette *et al*, 2010). To confirm the binding of SOCS1 and ATR, we performed Co-IP from MKN-45 cell lysate with an anti-ATR antibody. We confirmed the presence of SOCS1 and p53 in the Co-IP product by means of western blotting (Figure 3A), suggesting a combination of SOCS1, p53, and ATR. In an experiment in which ATR expression was knocked down via siRNA in SOCS1-transfected MKN-45 cells, there was no increase in p-Chk2 levels compared with SOCS1-transfected MKN-45 cells in which ATR expression was not knocked down (Figure 3B). By silencing ATR, a consistent increase in the ratio of SOCS1-

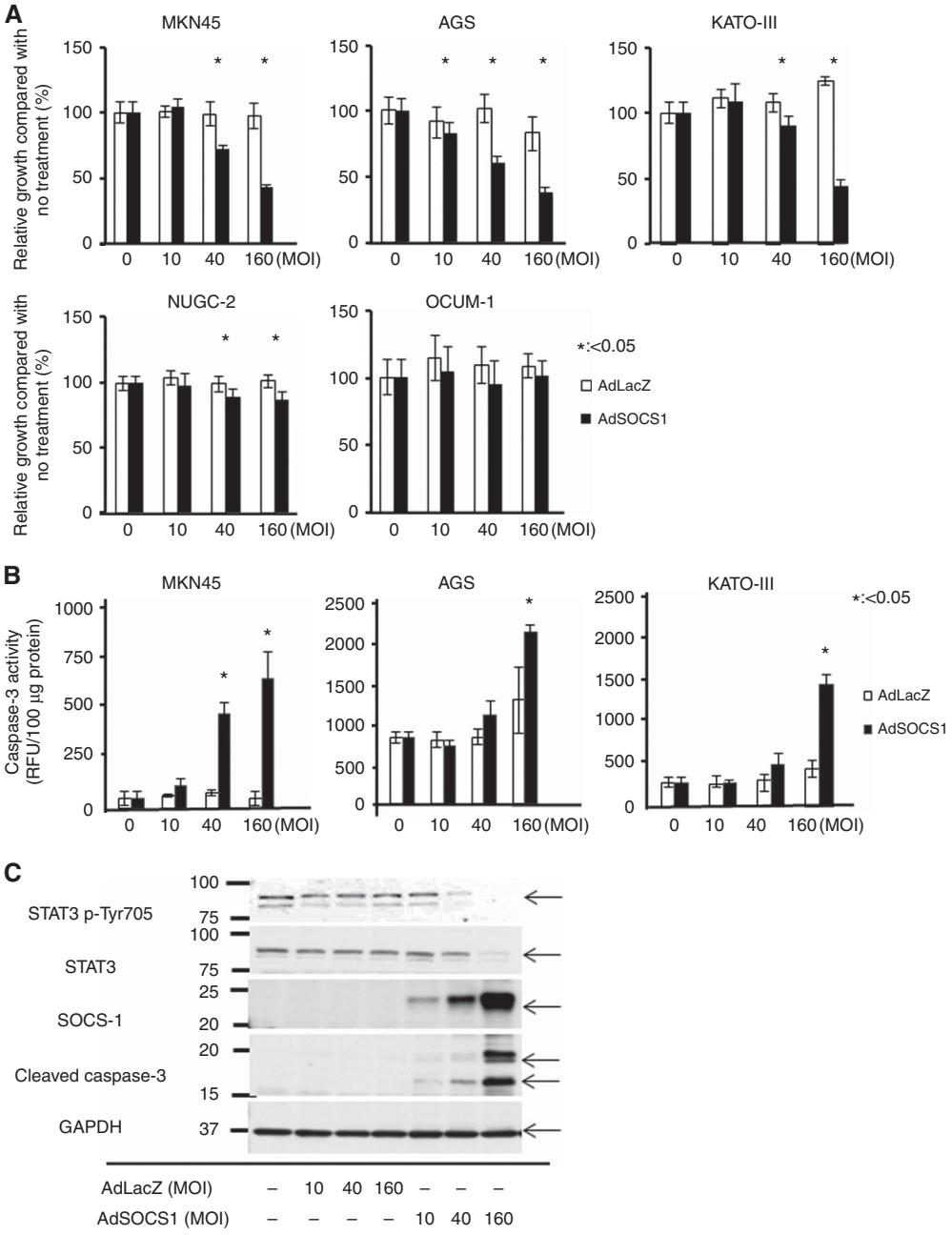

Figure 1. Overexpression of SOCS1 inhibits GC cell growth. (**A**) Effect of AdSOCS1 on viability of five GC cell lines. Cells were infected with either AdSOCS1 or AdLacZ (0–160 multiplicity of infection (MOI)). Growth ratios for AdLacZ- and AdSOCS1-infected cells were calculated as the percentage of absorbance readings for infected cells relative to that of untreated cells. Statistical analyses were performed using Welch's *t*-test and two-sided *P* values less than 0.05 were considered significant. Values shown represent the average ± standard deviation (s.d.) of hexaplicate wells. (**B**) Effect of AdSOCS1 on apoptosis. Activation of apoptosis was evaluated by caspase-3 fluorometric assay. Cells were infected with either AdSOCS1 or AdLacZ (0–160 MOI). After 48 h, enzymatic activity of caspase-3 was measured. Statistical analyses were performed using Welch's *t*-test and two-sided *P* values less than 0.05 were considered significant. Values shown represent average ± s.d. of triplicate wells. (**C**) Expression of SOCS1, phospho-STAT3, and cleaved caspase-3 after transduction of AdSOCS1.

transfected GC cells at the G2/M phase was restored in two GC cell lines (Figure 3C). Figure 3D shows a schema of the association between ATR and SOCS1 and their role in cell cycle regulation.

Antitumour activity of SOCS1 in a xenograft mouse model of peritoneal dissemination of human GC. We also evaluated the therapeutic effects of AdSOCS1 on the growth of tumours in an *in vivo* peritoneal dissemination model. Female ICR nu/nu mice were intraperitoneally transplanted with 3.0×10^6 cells of MKN45-Luc. The luminescence of these cells was monitored with the IVIS to determine whether tumour volume correlated with luminescent intensity. As the tumours grew, the luminescence intensity increased over time. Tumour volume was strongly correlated with the luminescence intensity emitted by the tumour, which was quantified using IVIS (Figure 4A). Figure 4B shows a schema of the protocol. To confirm the peritoneal dissemination models, the intraperitoneal tumour masses were visualised by bioluminescence imaging 21 days after the intraperitoneal injection. After confirming the validity of the dissemination model, we divided the mice into two groups: AdSOCS1 treatment and AdLacZ control. The

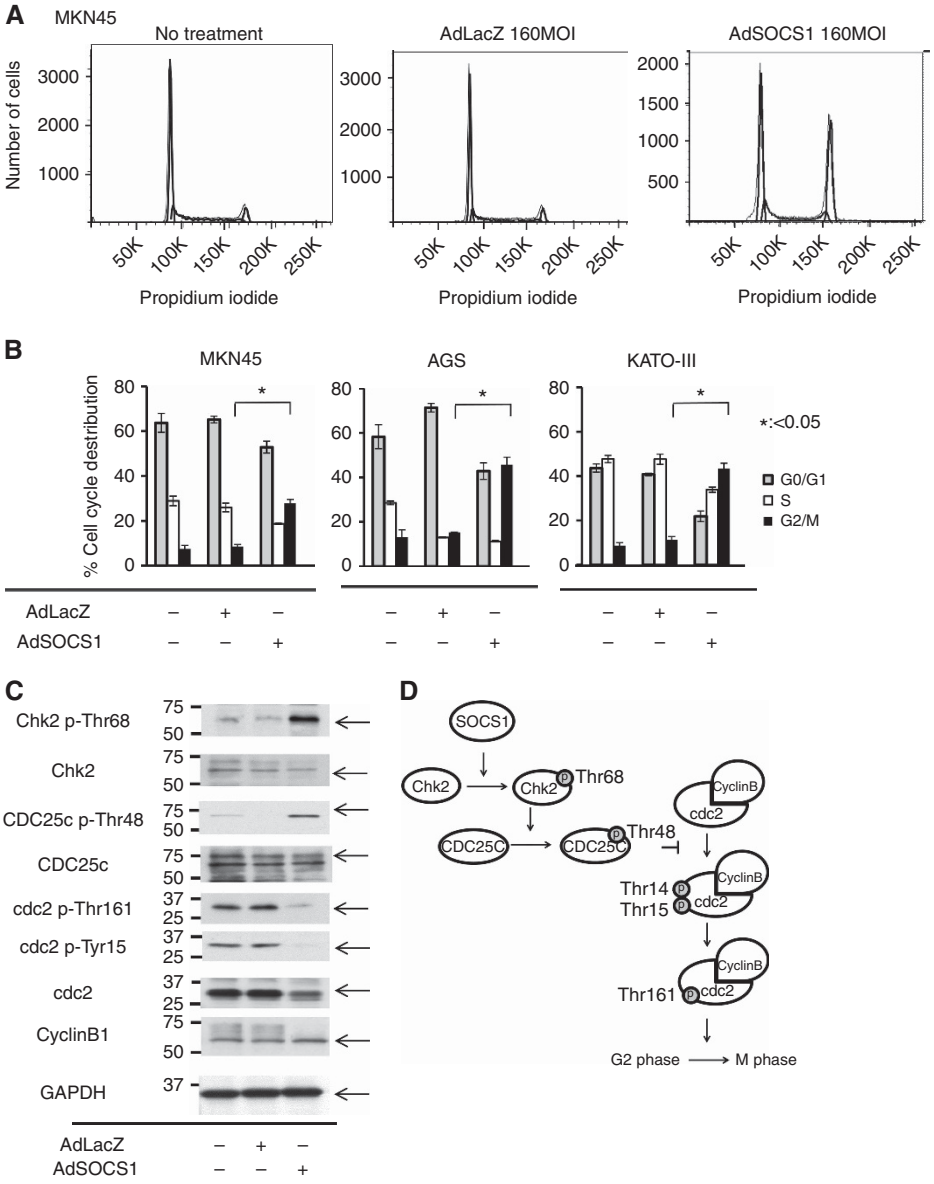

Figure 2. Effect of AdSOCS1 on cell cycle regulation in three GC cell lines. SOCS1 induced G2/M arrest in MKN45. Cells were infected with either AdSOCS1 or AdLacZ at 160 multiplicity of infection (MOI). After 24 h, cell cycle analysis was performed by flow cytometry with propidium iodide DNA staining. (**B**) SOCS1 induced G2/M arrest in GC cells. Cells were infected with either AdSOCS1 or AdLacZ at 160 MOI. After 24 h, cell cycle analysis was performed by flow cytometry with propidium iodide DNA staining. Statistical analyses were performed using Welch's *t*-test and two-sided *P* values less than 0.05 were considered significant. Values shown represent average ± s.d. of triplicate experiments. (**C**) SOCS1 phosphorylated chk2 and induced G2/M arrest. Cells were infected with either AdSOCS1 or AdLacZ at 160 MOI. After 48 h, whole cell lysates were prepared and immunoblotted with antibodies against cell cycle regulation proteins. (**D**) Schematic representation of cell cycle control at G2/M checkpoint.

mice were intraperitoneally treated with 1×10^8 pfu per 500 μl of AdSOCS1 or AdLacZ two times a week, a total of eight times from day 21 to day 49. We repeatedly measured the photon counts of the intraperitoneal tumour masses on days 35 and 49. Figure 4C shows a representative view of the changes in bioluminescence imaging in the two groups. Although the AdLacZ group showed an increase in bioluminescence, the AdSOCS1 group showed a decrease in bioluminescence. The total photon count in the AdSOCS1 group decreased gradually, whereas that of the AdLacZ group increased (Figure 4D). On day 49, the total photon count in the AdSOCS1 group was significantly lower than that of the control group (Figure 4E). Furthermore, the weight of the intraperitoneal tumour in AdSOCS1 group was significantly lower than that in the AdLacZ group (Figure 4F).

We also pathologically examined the therapeutic effects of AdSOCS1 on the growth of tumours *in vivo*. Immunohistochemical analysis revealed the overexpression of SOCS1 in tumours from the AdSOCS1 group (Figure 5A), and the expression of Ki-67 was significantly suppressed in the AdSOCS1 group compared with the AdLacZ group (Figure 5A). The peritoneally disseminated tumours were analysed by western blotting. In the AdSOCS1 group, we confirmed the expression of SOCS1 and decreased levels of pSTAT3 (Tyr705). Phosphorylation of Chk2 at Thr68, which is associated with cell cycle regulation, was also increased, the same as *in vitro* (Figure 5B). Terminal deoxynucleotidyl transferase dUTP nick end labeling staining showed that SOCS1 gene therapy induced apoptosis in the SOCS1-expressing area *in vivo* (Figure 5C).

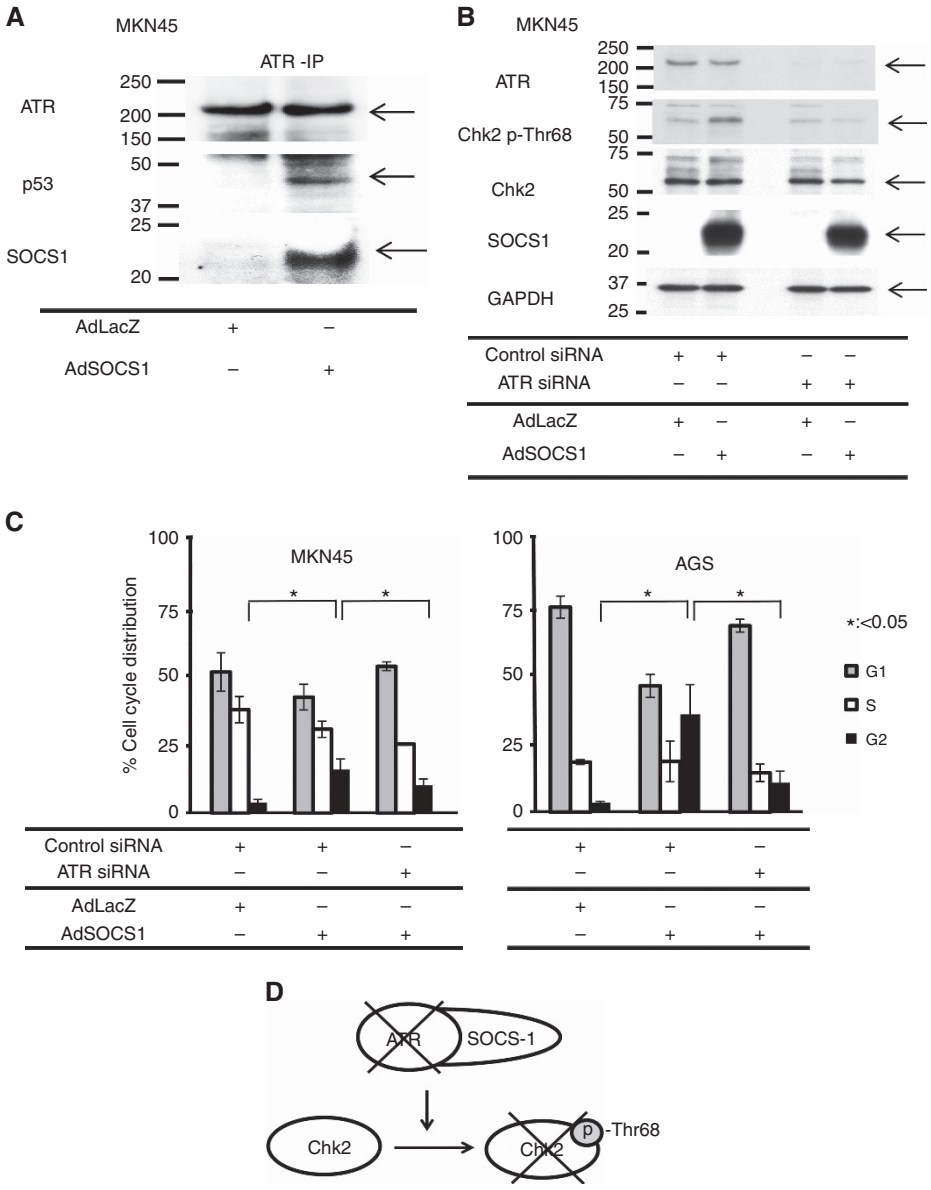

Figure 3. SOCS1 combined with ATR and activated the pathway of ATR-Chk2 cell cycle regulation. (**A**) SOCS1 interacted with ATR. MKN45 cells were infected with either AdSOCS1 or AdLacZ at 160 multiplicity of infection (MOI). Twenty-four hours after transfection, lysates were immunoprecipitated with anti-ATR antibody and immunoblotted with anti-SOCS1 and anti-p53 antibodies. (**B**) When ATR expression was suppressed by siRNA, phosphorylation of Chk2 was not increased by SOCS1. Twenty-four hours after transfection, cells were infected with either AdSOCS1 or AdLacZ as control (160 MOI). Twenty-four hours after infection, lysates were immunoblotted with anti-ATR, anti-phospho-Chk2, anti-total Chk2, and anti-SOCS1 antibodies. (**C**) SOCS1 did not induce G2/M arrest after ATR knockdown. MKN45 and AGS were transfected with control siRNA or siRNA against ATR. Twenty-four hours after transfection, cells were infected with either AdSOCS1 or AdLacZ as control (160 MOI). Twenty-four hours after infection, cell cycle analysis was performed by flow cytometry with propidium iodide DNA staining. Statistical analyses were performed using Welch's *t*-test and two-sided *P* values less than 0.05 were considered significant. Values shown represent average ± s.d. of triplicate experiments.

DISCUSSION

In a previous report, we showed in an *in vitro* experiment using GC cell lines that SOCS1 gene therapy leads to suppressed proliferation through JAK/STAT3 and p38 MAPK activation (Souma *et al*, 2012). However, the observed antitumour effect of SOCS1 was not fully explained by the combination of individual inhibitory effects, suggesting that other factors are involved. In the present study, we found that SOCS1 affected regulation of the cell cycle, a previously unrecognised effect of SOCS1 expression, in three GC cell lines. Cell cycle analysis of these cell lines revealed that the proportion of cells in the G2/M phase was increased, suggesting that SOCS1 was involved in cell cycle regulation, especially at the G2/M checkpoint. In cell cycle regulation, the G2/M checkpoint prevents cells with genomic DNA damage from entering into mitosis (M period) (Cuddihy and O'Connell, 2003; Dai and Grant, 2010; van Vugt and Yaffe, 2010). DNA damage activates checkpoint pathways and arrests the cell cycle to provide time for activation of DNA repair processes or to induce the apoptosis program. The activation of Chk2 phosphorylated at Thr68, which phosphorylates its substrates BRCA1, p53, Cdc25C, and Cdc25A, is involved in checkpoint arrest at the G1 and G2/M transitions (Gould and Nurse, 1989; Raleigh and O'Connell, 2000; Stolz *et al*, 2011).

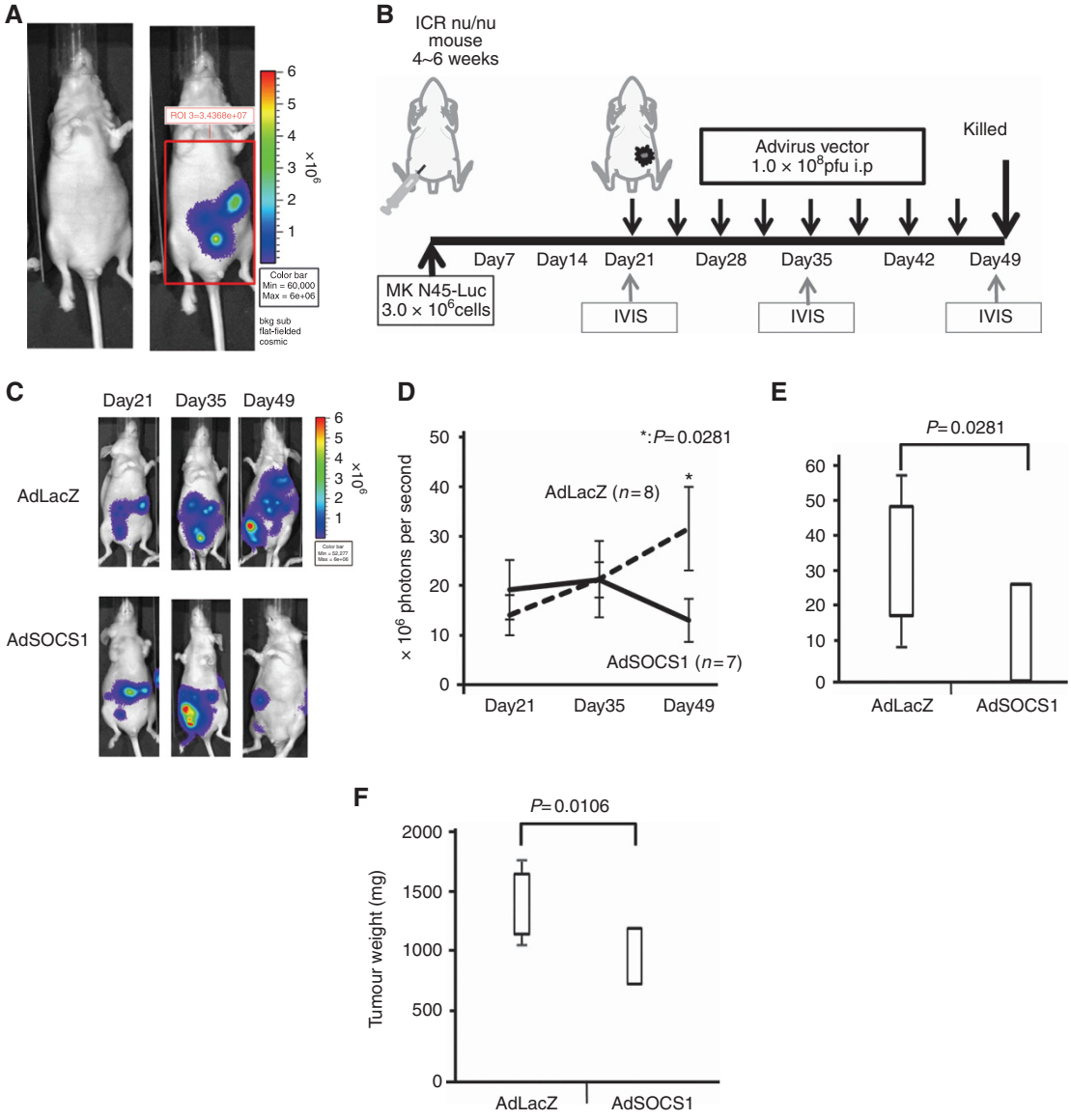

Figure 4. Antitumour effect of AdSOCS1 *in vivo*. (**A**) Peritoneal dissemination xenograft model with MKN45-Luc. Peritoneally disseminated tumours were detected with IVIS. (**B**) Schema of the protocol. Female ICR nu/nu mice were intraperitoneally transplanted with 3.0×10^6 MKN45-Luc cells. After confirmation of the peritoneal dissemination model, mice were intraperitoneally treated with AdSOCS1 or AdLacZ two times a week, eight times from day 21 to day 49. We repeatedly measured the photon counts of the intraperitoneal tumour masses on day 35 and day 49. (**C**) Two representative cases are shown. (**D**) Progression of disseminated tumour. Statistical analyses were performed using Mann–Whitney *U* test and two-sided *P* values less than 0.05 were considered significant. Values shown represent average ± s.e.m. (**E**) Photons were quantified by measuring the total counts over 20- and 25-min integration times and plotting relative to time. The total count of photons in the AdSOCS1 group was significantly higher than that in the AdLacZ group. (**F**) Weight of peritoneally disseminated tumours. All peritoneally disseminated tumours were collected. Values shown represent average weight ± s.d. Tumour weights in the AdSOCS1 group were significantly greater than those in the AdLacZ group. Statistical analyses were performed using Mann–Whitney *U* test and two-sided *P* values less than 0.05 were considered significant. Values shown represent average ± s.e.m.

Phosphorylated Cdc25C at Thr48 was reported to catalyse dephosphorylation of the Thr14 and Tyr15 residues in Cdc2. Moreover, activation of the Cdc2/cyclin B complex is maintained through phosphorylation at Thr161 and dephosphorylation at Thr14 and Tyr15 of Cdc2 (Figure 2D). In our study, the expression of SOCS1 in three GC cell lines (MKN45, AGS, and KATO-III) induced phosphorylation of Chk2 at Thr68 and Cdc25C at Thr48 and dephosphorylation of Cdc 2 at Tyr 15 and Tyr 161. On the basis of these results in checkpoint-related molecules, SOCS1 appears to be involved in the pathway, as shown in Figure 2D. However, the relationship between SOCS1 and Chk2 is still unknown.

ATR belongs to the phosphatidylinositol 3-kinase-related kinase protein family (Bentley *et al*, 2008). It is involved in sensing DNA damage and activating the DNA damage checkpoint, leading to cell cycle arrest (Sancar *et al*, 2004). ATR is activated in response to persistent single-stranded DNA, which is a common intermediate formed during DNA damage detection and repair. In this process, ATR was reported to activate the checkpoint kinases Chk1 and Chk2 (Brown and Baltimore, 2003). SOCS1 was reported to interact with ATR through the SOCS box (Calabrese *et al*, 2009; Mallette *et al*, 2010). Therefore, we first examined the interaction between SOCS1 and ATR *in vitro*, and we confirmed the binding of SOCS1 to ATR by Co-IP. Furthermore, following suppression of

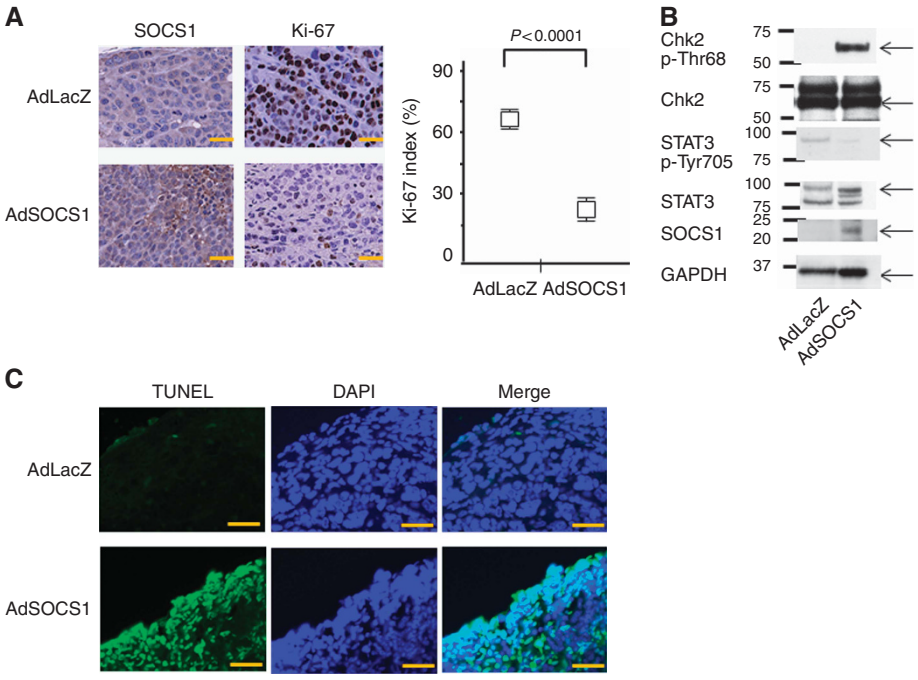

Figure 5. SOCS1 showed antitumour activity in a GC xenograft model: histological analysis of peritoneally disseminated tumours after SOCS1 gene therapy. (**A**) Immunohistochemical analysis of SOCS1 and Ki-67 in MKN45-Luc tissue from animals treated with AdSOCS-1 or AdLacZ. Scale bar = 20 μm. AdSOCS1 group showed increased SOCS1 expression in tumour and significantly decreased Ki-67 index. Ki-67 staining was recorded as the ratio of positively stained cells to all tumour cells in 10 fields (× 200 magnification). Statistical analyses were performed using Welch's *t*-test and two-sided *P* values less than 0.05 were considered significant. Values shown represent average ± s.d. (**B**) The peritoneally disseminated tumours treated with Ad-SOCS1 were analysed by western blotting. We confirmed the expression of SOCS1 and decreased levels of pSTAT3. Phosphorylation of Chk2 at Thr68 was also increased, the same as *in vitro*. (**C**) Immunohistochemical analysis by TUNEL (blue fluorescence, DAPI staining for nuclei; cyan fluorescence, TUNEL positive) in MKN45-Luc tissues from animals treated with AdSOCS1 or AdLacZ. Scale bar = 20 μm.

ATR, the effect of SOCS1 on the cell cycle was reduced, revealing a novel mechanism for SOCS1 antitumour effects through ATR.

Peritoneal carcinomatosis, the most frequent recurrent form of GC, is a mode of metastasis in which cancer cells penetrate through the gastric wall into the peritoneal cavity and grow on the peritoneum (Emoto *et al*, 2014; Imano and Okuno, 2014). Complete cure by surgery is difficult, and chemotherapy has been the first choice. However, chemotherapy for peritoneal dissemination is rendered inadequately efficacious owing to insufficient drug delivery, and patients have a poor prognosis, with symptoms such as intestinal obstruction and abdominal bloating. Currently, the safety and efficacy of intraperitoneal chemotherapy involving direct administration of a taxane-based anticancer drug into the peritoneal cavity is being tested in various clinical studies with a central focus on GC (Ishigami *et al*, 2009; Fujiwara *et al*, 2010; Ishigami *et al*, 2010; Fujiwara *et al*, 2012). Although multiple reports have suggested that the therapy may also be effective for GC, the details have yet to be revealed. In the present study, we studied the effects of SOCS1 gene therapy in five GC cell lines that can be used to create models of PC. Four of five GC cell lines showed antiproliferative effects, and only OCUM-1 did not show the effect. Because efficiency of adenoviral gene delivery into OCUM-1 was confirmed by using AdGFP (data not shown), proliferation of OCUM-1 might be little relation to JAKSTAT, p38MAPK, and ATR-Chk2 pathways, which associated with antiproliferative effects of SOCS1. Peritoneal carcinomatosis models were created using luciferase-transfected cells of the GC cell lines, upon which SOCS1 exerted an antitumour effect, allowing for evaluation of the therapeutic effect over time using IVIS. After intraperitoneal implantation, mice were divided into two groups and treated according to the protocols once IVIS-based evaluation of engrafted peritoneal nodules became possible. We found that this system was effective in the evaluation of therapeutic effects against PC, which is otherwise difficult. *In Vivo* Imaging System-based examination showed that the light intensity in the whole abdomen was significantly decreased in the treated group compared with the pretreatment level, whereas the light intensity increased in the control group. Furthermore, the significant difference in therapeutic effects was noted in terms of the post-treatment weight of the intra-abdominal tumour. On the basis of these results, we deemed the therapy to be effective. Furthermore, pathological examination by double immunostaining showed that SOCS1 and TUNEL staining were superimposable, suggesting that introduced SOCS1 directly affects cells. Moreover, because we confirmed that SOCS1 also affected the phosphorylation of Chk2 in Figure 5B, SOCS1 may induce G2/M cell arrest in these PC models.

The total photon count and tumour weight of the SOCS1-treated mice were significantly suppressed, indicating the effectiveness of the therapy. However, all pathological examinations of the tumours underwent SOCS1 therapy showed residual cancer cells in this study, indicating that a cure is difficult to achieve for greater nodules with only SOCS1 therapy. From the findings that we seldom observed uptake into deeper regions, it may be a limitation of intraperitoneally administered therapy. A cure may be achievable if patients' disease is limited to microdissemination at an earlier stage in clinical settings. Furthermore, repetitive treatments may be expected to be effective. Although systemic administration of SOCS1 is likely difficult because of possible adverse events due to suspected systemic inhibitory effects on signalling pathways, mainly on JAK/STAT, this study supports the potential of administration in a limited area, such as the peritoneal cavity, whereby the localised effect would be expected to occur in a limited area.

Because of the very efficient nuclear entry mechanism of adenovirus and its low pathogenicity for humans, adenovirus-based

vectors have become gene delivery system especially for cancer gene therapy (Nishizaki *et al*, 1999). However, using adenovirus was reported to be risky in that too high dose that resulted in acute toxicity (Gao *et al*, 1996). Although side effects have been mild in adenoviral therapy in these days, and this therapy is mainly limited in abdominal cavity, side effects should consistently be monitored in patients, particularly in the liver at the clinical application.

In this study, we discovered a novel antitumour mechanism for SOCS1 treatment of GC based on cell cycle arrest. Furthermore, we confirmed the antitumour effects of SOCS1 in a peritoneal dissemination mouse model. We intend to explore the possibility of viral therapy further in the form of intraperitoneal chemotherapy combined with conventional chemotherapy for clinical applications in humans.

ACKNOWLEDGEMENTS

This work was supported by a Grant-in-Aid from the Ministry of Health, Labour and Welfare, Japan (T Naka) and a grant from the Kansai Biomedical Cluster Project in Saito, which is promoted by the Knowledge Cluster Initiative of the Ministry of Education, Culture, Sports, Science and Technology, Japan (T Naka). We are grateful to Ms M Ako for experimental assistance and Ms Y Kanazawa and Ms J Yamagishi for secretarial assistance.

REFERENCES

Bentley NJ, Holtzman DA, Flaggs G, Keegan KS, DeMaggio A, Ford JC, Hoekstra M, Carr AM (2008) The Schizosaccharomyces pombe rad3 checkpoint gene. *Clin Transl Oncol* **10**: 538–542.

Brown EJ, Baltimore D (2003) Essential and dispensable roles of ATR in cell cycle arrest and genome maintenance. *Genes Dev* **17**: 615–628.

Calabrese V, Mallette FA, Deschênes-Simard X, Ramanathan S, Gagnon J, Moores A, Ilangumaran S, Ferbeyre G (2009) SOCS1 links cytokine signaling to p53 and senescence. *Mol Cell* **36**: 754–767.

Cuddihy AR, O'Connell MJ (2003) Cell-cycle responses to DNA damage in G2. *Int Rev Cytol* **222**: 99–140.

Dai Y, Grant S (2010) New insights into checkpoint kinase 1 in the DNA damage response signaling network. *Clin Cancer Res* **16**: 376–383.

Emoto S, Sunami E, Yamaguchi H, Ishihara S, Kitayama J, Watanabe T (2014) Drug development for intraperitoneal chemotherapy against peritoneal carcinomatosis from gastrointestinal cancer. *Surg Today* **44**: 2209–2220.

Ferlay J, Shin HR, Bray F, Forman D, Mathers C, Parkin DM (2010) Estimates of worldwide burden of cancer in 2008: GLOBOCAN 2008. *Int J Cancer* **127**: 2893–2917.

Fujimoto M, Naka T (2003) Regulation of cytokine signaling by SOCS family molecules. *Trends Immunol* **24**: 659–666.

Fujiwara Y, Nishida T, Takiguchi S, Nakajima K, Miyata H, Yamasaki M, Yamamoto K, Moon JH, Mori M, Doki Y (2010) Feasibility study of S-1 and intraperitoneal docetaxel combination chemotherapy for gastric cancer with peritoneal dissemination. *Anticancer Res* **30**: 1335–1339.

Fujiwara Y, Takiguchi S, Nakajima K, Miyata H, Yamasaki M, Kurokawa Y, Mori M, Doki Y (2012) Intraperitoneal docetaxel combined with S-1 for advanced gastric cancer with peritoneal dissemination. *J Surg Oncol* **105**: 38–42.

Gao GP, Yang Y, Wilson JM (1996) Biology of adenovirus vectors with E1 and E4 deletions for liver-directed gene therapy. *J Virol* **70**: 8934–8943.

Gould KL, Nurse P (1989) Tyrosine phosphorylation of the fission yeast cdc2 + protein kinase regulates entry into mitosis. *Nature* **342**: 39–45.

Imano M, Okuno K (2014) Treatment strategies for gastric cancer patients with peritoneal metastasis. *Surg Today* **44**: 399–404.

Ishigami H, Kitayama J, Kaisaki S, Hidemura A, Kato M, Otani K, Kamei T, Soma D, Miyato H, Yamashita H, Nagawa H (2010) Phase II study of weekly intravenous and intraperitoneal paclitaxel combined with S-1 for advanced gastric cancer with peritoneal metastasis. *Ann Oncol* **21**: 67–70.

Ishigami H, Kitayama J, Otani K, Kamei T, Soma D, Miyato H, Yamashita H, Hidemura A, Kaisaki S, Nagawa H (2009) Phase I pharmacokinetic study of weekly intravenous and intraperitoneal paclitaxel combined with S-1 for advanced gastric cancer. *Oncology* **76**: 311–314.

Iwahori K, Serada S, Fujimoto M, Ripley B, Nomura S, Mizuguchi H, Shimada K, Takahashi T, Kawase I, Kishimoto T, Naka T (2013) SOCS-1 gene delivery cooperates with cisplatin plus pemetrexed to exhibit preclinical antitumor activity against malignant pleural mesothelioma. *Int J Cancer* **132**: 459–471.

Koizumi W, Narahara H, Hara T, Takagane A, Akiya T, Takagi M, Miyashita K, Nishizaki T, Kobayashi O, Takiyama W, Toh Y, Nagaie T, Takigi S, Yamamura Y, Yanaoka K, Orita H, Takeuchi M (2008) S-1 plus cisplatin versus S-1 alone for first-line treatment of advanced gastric cancer (SPIRITS trial): a phase III trial. *Lancet Oncol* **9**: 215–221.

Mallette FA, Calabrese V, Ilangumaran S, Ferbeyre G (2010) SOCS1, a novel interaction partner of p53 controlling oncogene-induced senescence. *Aging* **2**: 445–452.

Maruyama K, Kaminishi M, Hayashi K, Isobe Y, Honda I, Katai H, Arai K, Kodera Y, Nashimoto A (2006) Gastric cancer treated in 1991 in Japan: data analysis of nationwide registry. *Gastric Cancer* **9**: 51–66.

Mizuguchi H, Kay MA (1999) A simple method for constructing E1- and E1/E4-deleted recombinant adenoviral vectors. *Hum Gene Ther* **10**: 2013–2017.

Nishizaki M, Fujiwara T, Tanida T, Hizuta A, Nishimori H, Tokino T, Nakamura Y, Bouvet M, Roth JA, Tanaka N (1999) Recombinant adenovirus expressing wild-type p53 is antiangiogenic: a proposed mechanism for bystander effect. *Clin Cancer Res* **5**: 1015–1023.

Oshimo Y, Kuraoka K, Nakayama H, Kitadai Y, Yoshida K, Chayama K, Yasui W (2004) Epigenetic inactivation of SOCS-1 by CpG island hypermethylation in human gastric carcinoma. *Int J Cancer* **112**: 1003–1009.

Parkin DM, Bray F, Ferlay J, Pisani P (2005) Global cancer statistics, 2002. *CA Cancer J Clin* **55**: 74–108.

Parrillas V, Martínez-Muñoz L, Holgado BL, Kumar A, Cascio G, Lucas P, Rodríguez-Frade JM, Malumbres M, Carrera AC, van Wely KH, Mellado M (2013) Suppressor of cytokine signaling 1 blocks mitosis in human melanoma cells. *Cell Mol Life Sci* **70**: 545–558.

Pasini F, Fraccon AP, DE Manzoni G (2011) The role of chemotherapy in metastatic gastric cancer. *Anticancer Res* **31**: 3543–3554.

Raleigh JM, O'Connell MJ (2000) The G(2) DNA damage checkpoint targets both Wee1 and Cdc25. *J Cell Sci* **113**: 1727–1736.

Sancar A, Lindsey-Boltz LA, Unsal-Kaçmaz K, Linn S (2004) Molecular mechanisms of mammalian DNA repair and the DNA damage checkpoints. *Annu Rev Biochem* **73**: 39–85.

Shimada K, Serada S, Fujimoto M, Nomura S, Nakatsuka R, Harada E, Iwahori K, Tachibana I, Takahashi T, Kumanogoh A, Kishimoto T, Naka T (2013) Molecular mechanism underlying the antiproliferative effect of suppressor of cytokine signaling-1 in non-small-cell lung cancer cells. *Cancer Sci* **104**: 1483–1491.

Souma Y, Nishida T, Serada S, Iwahori K, Takahashi T, Fujimoto M, Ripley B, Nakajima K, Miyazaki Y, Mori M, Doki Y, Sawa Y, Naka T (2012) Antiproliferative effect of SOCS-1 through the suppression of STAT3 and p38 MAPK activation in gastric cancer cells. *Int J Cancer* **131**: 1287–1296.

Stolz A, Ertych N, Bastians H (2011) Tumor suppressor CHK2: regulator of DNA damage response and mediator of chromosomal stability. *Clin Cancer Res* **17**: 401–405.

Takahashi T, Serada S, Ako M, Fujimoto M, Miyazaki Y, Nakatsuka R, Ikezoe T, Yokoyama A, Taguchi T, Shimada K, Kurokawa Y, Yamasaki M, Miyata H, Nakajima K, Takiguchi S, Mori M, Doki Y, Naka T, Nishida T (2013) New findings of kinase switching in gastrointestinal stromal tumor under imatinib using phosphoproteomic analysis. *Int J Cancer* **133**: 2737–2743.

To KF, Chan MW, Leung WK, Ng EK, Yu J, Bai AH, Lo AW, Chu SH, Tong JH, Lo KW, Sung JJ, Chan FK (2004) Constitutional activation of IL-6-mediated JAK/STAT pathway through hypermethylation of SOCS-1 in human gastric cancer cell line. *Br J Cancer* **91**: 1335–1341.

Toyoshima M, Tanaka Y, Matumoto M, Yamazaki M, Nagase S, Sugamura K, Yaegashi N (2009) Generation of a syngeneic mouse model to study the intraperitoneal dissemination of ovarian cancer with in vivo luciferase imaging. *Luminescence* **24**: 324–331.

van Cutsem E, Moiseyenko VM, Tjulandin S, Majlis A, Constenla M, Boni C, Rodrigues A, Fodor M, Chao Y, Voznyi E, Risse ML, Ajani JA (2006) Phase III study of docetaxel and cisplatin plus fluorouracil compared with cisplatin and fluorouracil as first-line therapy for advanced gastric cancer: a report of the V325 Study Group. *J Clin Oncol* **24**: 4991–4997.

van Vugt MA, Yaffe MB (2010) Cell cycle re-entry mechanisms after DNA damage checkpoints: giving it some gas to shut off the breaks! *Cell Cycle* **9**: 2097–2101.

Watanabe D, Ezoe S, Fujimoto M, Kimura A, Saito Y, Nagai H, Tachibana I, Matsumura I, Tanaka T, Kanegane H, Miyawaki T, Emi M, Kanekura Y, Kawase I, Naka T, Kishimoto T (2004) Suppressor of cytokine signalling-1 gene silencing in acute myeloid leukaemia and human haematopoietic cell lines. *Br J Haematol* **126**: 726–735.

Xu Y, Wang W, Gou A, Li H, Tian Y, Yao M, Yang R (2015) Effects of suppressor of cytokine signaling 1 silencing on human melanoma cell proliferation and interferon-γ sensitivity. *Mol Med Rep* **11**: 583–588.

Supplementary Information accompanies this paper on British Journal of Cancer website (http://www.nature.com/bjc)